

# Experimental Investigation and Modeling of the Heat Transfer Coefficient in the Pool Boiling: Bubble Dynamic and Artificial Intelligence

**Khooshehchin, Mohsen; Mohammadidoust, Akbar\***<sup>+</sup>

*Department of Chemical Engineering, Kermanshah Branch, Islamic Azad University, Kermanshah, I.R. IRAN*

**ABSTRACT:** In this work, the heat transfer coefficient in the pool boiling process was investigated for different alcoholic solutions. To exact evaluation, the bubble dynamic including bubble departure diameter, bubble departure frequency, and active nucleation sites' density were studied. The results showed that with increasing isopropanol concentration (20 V.% - 80 V.%), bubble departure frequency and active nucleation sites increased while bubble departure diameter decreased. The bubble dynamic cannot be effective in any amount and must be optimized to reach an optimum heat transfer coefficient. Isopropanol concentration of 20 V.% was reported as an optimum state and lower decrease versus deionized water (11.892%). This result confirmed that the bubble departure diameter played a significant role in promoting the heat transfer coefficient. Finally, to predict the experimental data, a Genetic Algorithm (GA) based correlation (power-law function) was developed. The optimization procedure revealed that the GA model had a good agreement with the experimental data ( $R^2=0.968$ ,  $AAD=0.0288$ ). In addition, this approach was compared with conventional models (Palen, Stephan, Unal, Fujita, and Inoue). The GA and the Stephan models presented the best and worst performance, respectively.

**KEYWORDS:** Bubble dynamic; Heat transfer coefficient; Pool boiling; Optimization; Genetic algorithm.

## INTRODUCTION

Energy management, both in production and transmission in systems that deal with large volumes of thermal energy, has a special importance due to the global energy crisis. In a system, an efficient evaporator can reduce energy consumption, economic resources, and dangers to the environment [1]. In addition, energy management in terms of heat loss at different processes requires a better performance in the process to increase efficiency, optimization and safety of the involved

equipments, simultaneously [2, 3]. The performance of devices in many applications is dependent on their ability to improve heat transfer [4]. Phase change processes are still of interest in the field of thermal management due to their inherent advantages in providing energy and uniform temperature distribution on the surfaces [5]. The nucleate boiling process is a complex process that is associated with phase change and affected by many factors such as fluid properties, operating pressure, and heat transfer

\* To whom correspondence should be addressed.

+ E-mail: mohammadidoust@gmail.com & mohammadidoust@iauksh.ac.ir  
1021-9986/2022/10/3376-3389 14/\$6.04

surface's conditions [6, 7]. Heat transfer in pool boiling can provide very high amounts of heat in low superheated conditions due to the latent heat of evaporation of the fluid during the phase transfer process [8]. Existence of high evaporation latent heat and bubble dynamic properties, including bubble departure frequency, bubble departure diameter and density of active nucleation sites make the nucleate boiling process superior than other heat transfer modes [9]. Due to its simplicity and passive operation, pool boiling is used to transfer heat in the nuclear reactors, electronic cooling, steam power plants, processing industries, etc. [10]. Boiling performance is usually determined by two parameters, Boiling Heat Transfer Coefficient (BHTC) and Critical Heat Flux (CHF) [11, 12]. The thermal performance of the equipment is limited to the CHF point, which is the point at which the nucleate boiling curve is transferred to the film boiling, which is characterized by drying at the heat transfer surface [6]. At the CHF point, a sudden temperature increase, occurs on the surface and then drastically declines the heat transfer rate and causes a corrosion on the heating surface [13]. Because at the CHF, a layer of steam (resistant layer) is formed on the hot surface, so the heat transfer performance is greatly decreased [14]. In addition, the CHF is a critical parameter related to the safety performance of the heat transfer surface [15]. The CHF models for the pool boiling have been presented in the literature [16-18]. The mechanisms can be summarized to increasing the heat transfer surface, increasing active nucleation sites, surface moisture capability and dynamic bubble modulation, such as bubble departing frequency [19]. Meanwhile, during the boiling process, the bubble departure frequency and bubble departure diameter are the main parameters for predicting the BHTC in many experimental correlations [20, 21]. Porous foam [22, 23], surface roughening [24, 25], magnetic fields (MFs) [26-28], electric field (EF) [29, 30], microporous coating [31, 32], use fins [33, 34], change the angle of the heat transfer surface [35, 36] are some of methods to increase the BHTC by increasing the bubble dynamics.

A number of models for predicting the BHTC for different solutions have been obtained since 1950 based on laboratory data. Palen [37] offered the first model for a liquid mixture in 1964. In this model, the BHTC was assumed as a function of temperature as exponential form. In 1969, Stephan and Körner [38] introduced their model, which is

one of the most important relations in predicting the BHTC. This model has a regulating parameter that has increased its range of application for liquid mixtures. One of the prominent features of this modeling was the possibility of extrapolation in predicting the BHTC in the amount of high heat fluxes. More models have been presented in the literature [39-46].

The mathematical form of the BHTC prediction models for pure solution and multicomponent solutions have been tabulated in Appendix A.

The main aim of this work is the investigation of bubble dynamic (bubble departure diameter, bubble departure frequency and bubble nucleation site's density) for attaining a good evaluation in determining the heat transfer coefficient of the pool boiling. In addition, it can be found from the literature that the artificial intelligence have rarely been employed in the pool boiling process. Therefore, in this work, we tried to introduce a powerful model based on Genetic Algorithm (GA) correlation for predicting the BHTC according to the experimental data with high accuracy in comparison with the previous models.

## EXPERIMENTAL AND THEORETICAL SECTION

### Set up

Fig. 1 illustrates the experimental set up used in this work. The system under test consists of a metal cylinder heater (heat transfer surface) made of copper with a fixed roughness of 0.95 micrometers. Cylindrical heater has outer and inner diameters of 22 and 12 mm, respectively. In addition, its length is 160 mm. In the center of this cylinder, a pencil lamp with a power of 1 kW (Osram lamp, Germany) to generate heat was used. The heater was placed in the center and bottom of a glass container, so that the solution surrounds it. This glass container has a high thermal resistance and thickness of 10 mm. This vessel was surrounded by some glass wool to avoid heat losses. Moreover, its dimensions including width, length and height are 40, 160 and 300 mm, respectively. To turn on the lamp and generate heat, the lamp was connected to a 1 kW autotransformer capable of changing the voltage in the range of 0 - 300 V. To measure the surface temperature, three holes with a diameter of 2 mm at an angle of 120 to each other in the nearest part on the outer surface of the heater. We made inside each of the holes a K-type thermocouple with a range of -180 °C to +750 °C and high sensitivity.

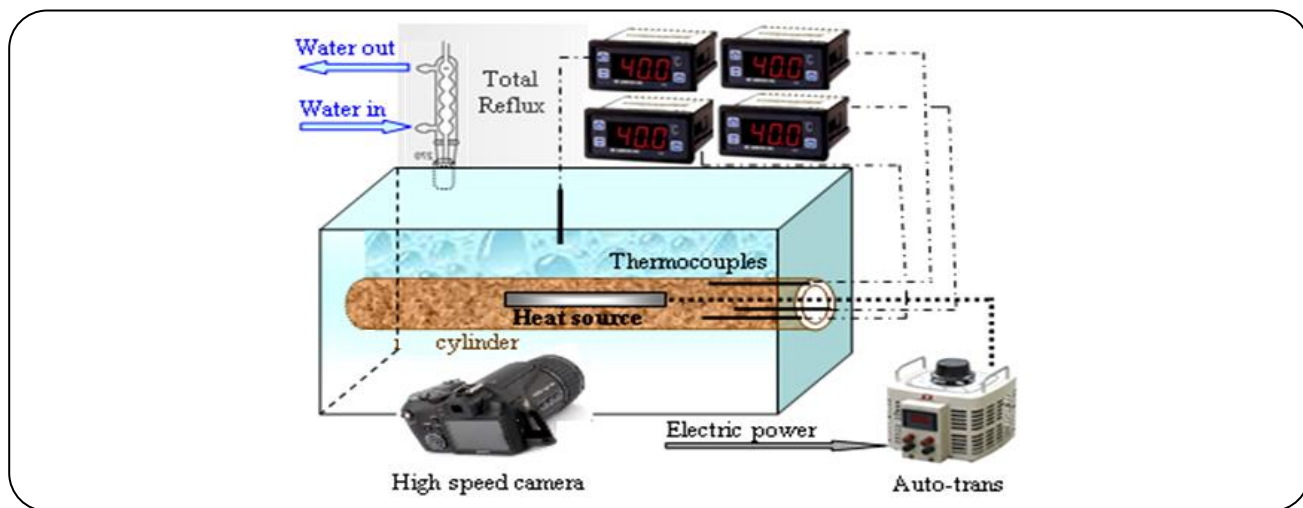


*Fig. 1: Schematic view of the experimental apparatus.*

### Experimental procedure and analyses

The test vessel containing two liters of the solution (water and isopropanol) was heated to boiling point by an auto-trans. After reaching the saturated boiling, the solution remains in this state for half an hour. This time allows air bubbles to escape from the liquid phase and the heater's surface. First, experiments were started with deionized water as the base solution and then followed by isopropanol solutions (step of 20 V.%). To ensure that it was at saturation boiling condition, the fourth thermocouple was employed. The voltage range was increased from 30 to 240 V by auto-trans (step of 30 V). It took 5 min to change the voltage (stable state). At each stage of the experiments, for recording the boiling process, a Sony PMW-300K1 high-speed video camera was utilized. Subsequently, bubble dynamics' changes including the bubble departure frequency (by counting output bubbles per unit time), the bubble departure diameter (by averaging the diameter of a certain number of bubbles' output) as well as active nucleation sites (number of generating points per unit area) were investigated by slowing down the recorded films in EDIUS software (film editing software). Finally, A viscometer (kp0312 model, Iran) was employed with a U shaped cell in a glycerin bath fixed at specified temperature ( $\pm 0.02$  °C) for measuring the kinematic viscosity of the solution. The viscosity was measured at the range of 20-500 °C. It should be noted that each experiment was repeated at least 3 times and the average of the experimental data was taken into account. More details of the device are shown in Fig. 1.

### Uncertainty and data reduction

The uncertainty of heat transfer coefficient can be determined by the Newton cooling law:

$$h = \frac{q/A}{(T_s - T_{sat})} \quad (1)$$

Heat flux was calculated by the following equation:

$$q/A = V \cdot I / A \cdot \cos\varphi \quad (2)$$

The  $\cos\varphi$  was assumed to be equal to unity, because of the linear shape of heater section and the absence of any solenoid effect. The maximum estimated uncertainty of heat flux would be based on Eq. (3) [47]:

$$\frac{\delta(q/A)}{q/A} = \sqrt{\left(\frac{\delta I}{I}\right)^2 + \left(\frac{\delta V}{V}\right)^2} \quad (3)$$

Before calculating the uncertainty for heat transfer coefficient,  $\delta h$ , it is necessary to determine the uncertainty of temperature difference,  $\delta\Delta T$  by the following [47]:

$$\delta\Delta T = \sqrt{(\delta T_s)^2 - (\delta T_{th})^2} \quad (4)$$

$$\frac{\delta h}{h} = \sqrt{\left(\frac{\delta I}{I}\right)^2 + \left(\frac{\delta V}{V}\right)^2 + \left(\frac{\delta T}{T}\right)^2} \quad (5)$$

Since the exact recording of the heater surface temperature by thermocouple is important for analyzing the results and, on the other hand, the places of the thermocouples' installation are in small distance from the outer surface of the heater and this small spacing

causes trivial difference in recording the real temperature, Eq. (6) was used to correct this temperature error:

$$T_S = T_{th} - \frac{q'' b_s}{K_s} \quad (6)$$

In this equation,  $b_s$  is the distance between the thermocouple locations and the heat transfer surface and  $K_s$  is the thermal conductivity of the heater material

The average temperature of three thermocouples ( $\bar{T}_S$ ) was calculated from Eq. (7):

$$\bar{T}_S = \frac{1}{n} \sum_{i=1}^n T_{S,i} \quad (7)$$

The accuracies of the uncertainty analysis for the experiments carried out, are tabulated in Table 1.

#### Device validation

To verify the functionality and accuracy of the laboratory apparatus before starting the data gathering, several tests were performed by deionized water as the base fluid. Then the results were compared with the three popular models of *Rohsenow* [20], *Stephan and Abdelsalam* [21] and *Gorenflo* [48]. Fig. 2 shows the validation of the experimental rig. Concerning this figure, it can be found that there is a proper validation at three times of the experiments. In addition, the experimental data have a good agreement with the conventional model, especially *Rohsenow* model.

Moreover, in order to reduce the effect of hysteresis phenomena and minimize its error, experiments (deionized water) were performed twice from bottom-up heat flux and twice from top-down heat flux (Fig. 3).

The results of the experiments in Fig. 3 show that when the experiments were performed from low to high voltage, higher values of the boiling heat transfer coefficient were obtained. But lower values were determined from high to low ones. The reason for this decrease is the filling of the active bubble generating points on the heat transfer surface at higher heat fluxes. As a result, all experiments in this study were carried out with a voltage increase trend.

#### Data analysis

Modeling is an important approach that can assist in the quick prediction of process response. It can reduce the number of experiments as well as the cost and time. In this work, the heat transfer coefficient was considered

**Table 1: Uncertainty sources.**

Parameter	Uncertainty
Tube diameter	$\pm 0.01$ mm
Tube length	$\pm 0.01$ mm
Thermocouple, K-type	$\pm 0.1$ °C
Voltage	$\pm 1$ V
Current	$\pm 0.1$ A
pH meter	$\pm 0.01$
maximum heat flux of $76 \text{ kW m}^{-2}$	$\pm 1.8545 \text{ kW m}^{-2}$

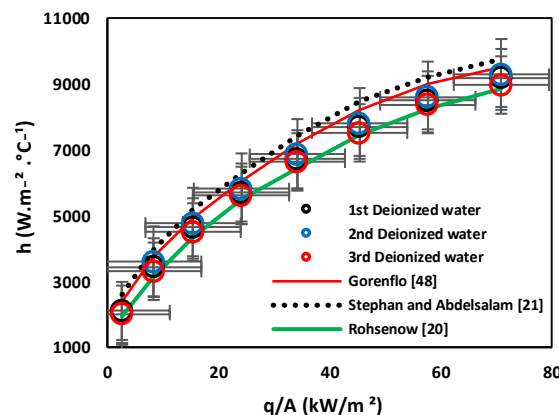


**Fig. 2: The validation of the experimental rig and comparison with conventional models.**

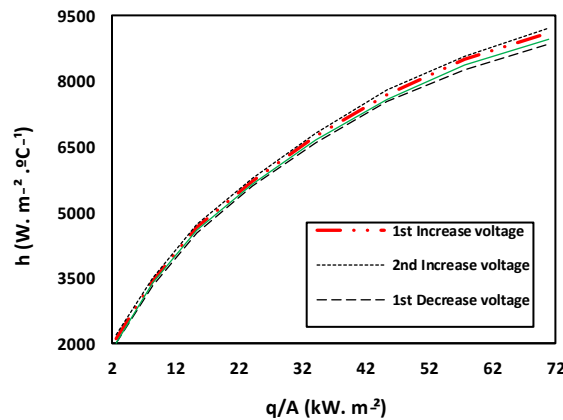


**Fig. 3: Comparison of the ratio of changes in boiling heat transfer coefficient with increasing and decreasing voltage.**

As the output of the process. To exact evaluation, heat parameter, bulk temperature, density (liquid and vapor), thermal conductivity, enthalpy, surface tension, heat capacity and thermal diffusion coefficient were regarded as the input of the process. According to the parameters

**Table 2: The range of data used in the GA.**

Parameter	Type	Min	Max
$q''$	input	2.6557	78.219
$T_{bulk}$	input	356.15	373.15
$\rho_l$	input	851.7489	959.6350
$\rho_v$	input	0.6288	1.2855
$k_l$	input	0.2375	0.6704
$h_{fg}$	input	1655383	2345214
$\sigma$	input	0.01944	0.05813
$C_{pl}$	input	3933.62	4361.49
$\alpha'_l$	input	605.3387	9023.4933
$h$	output	627.592	7020.88

mentioned above and power-law equation, a GA based correlation was presented. Finally, the suggested model was compared to other models in the literature. Table 2 reports the range of experimental data used in this work.

### Genetic algorithm

Genetic Algorithm (GA) is the other subset of the artificial intelligence and is a numerical solution for obtaining optimum response (maximum or minimum) especially in non-linear problems. In general, GA carries out a quick movement to search probability solutions in problem space. Proper responses are randomly determined and without expanding all the states. GA is a special type of evolution algorithm that uses the biological techniques such as inheritance and mutation. It was first presented by *John Henry Holland* [48]. In fact, GA uses Darwin's natural selection principles to find the optimal formula and matching with the desired pattern. It is often a good tool for regression-based prediction techniques [49]. According to the experimental results, a correlation among the heat transfer coefficient and independent variables is determined by GA optimizer. A power-law function is assumed as follows. It is inspired by the models in Appendix A.

$$h = \left( \frac{q \times I^*}{k_l \times T_{bulk}} \right)^{g_0} \left( \frac{\alpha'^2 \times \rho_l}{\sigma_{min} \times I^*} \right)^{g_1} \times \\ \left( \frac{C_{pl} \times T_{bulk} \times I^{*2}}{\alpha'^2} \right)^{g_2} \times \left( \frac{h_{fg} \times I^{*2}}{\alpha'^2} \right)^{g_3} \times \left( \frac{\rho_v}{\rho_l} \right)^{g_4} \quad (8)$$

Where,

$$I^* = \left( \frac{\sigma}{g(\rho_l - \rho_v)} \right)^{0.5} \quad (9)$$

In this study, the optimum constant values ( $g_i$ ) are found through the experimental variables based on GA. Desired GA of the work was attained by MATLAB software (R2014a).

### RESULTS AND DISCUSSION

In this section and in the first part, the experiments were carried out with the optimization of the boiling heat transfer coefficient through examining the behavior of the bubble dynamic parameters. The dynamic parameters of the bubble (Bubble departure diameter, Bubble departure frequency and Active nucleation sites' density) can increase the mixing state in the solution and thus increase the BHTC. Of course, increasing these parameters must be optimal. This means that the dynamic parameters cannot be increased to any extent because they may create a bubble layer on the heat transfer surface and reduce the BHTC [50]. The experiments were performed with deionized water and continued with the addition of isopropanol until a isopropanol 80 V.% of solution was obtained. After experimental optimization and obtaining the results, a GA based correlation was introduced and compared with previous models to predict the heat transfer coefficient. Finally, it is introduced to the best model that has the best overlap with laboratory results.

### The bubble dynamic's effects on the heat transfer coefficient, experimentally

Fig. 4 illustrates the variations in the BHTC from deionized water to 80 V.%, by step of 20% V.

As shown in the figure, deionized water was able to achieve the highest heat transfer coefficient with an upward trend and then decreasing procedure was observed

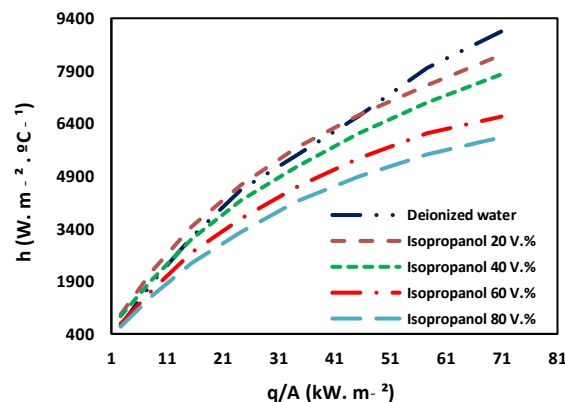


Fig. 4: The variations of the BHTC at different solutions.

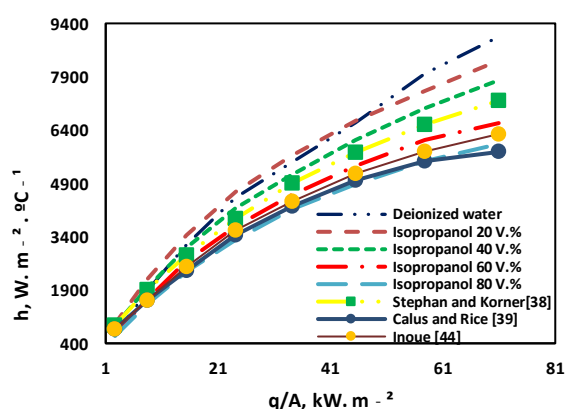


Fig. 5: The validation of the BHTC at different solutions.

with adding the isopropanol. Variations (versus deionized water) for 20 V.% and 80 V.% of isopropanol were determined to be 11.892% (min) and 23.871% (max), respectively. The slope of the curves was higher in low heat fluxes than high heat fluxes. This decrease in the BHTC can be attributed to the increase in their volatility and the decrease in surface tension of the solution due to the addition of the isopropanol [51-53]. The validation of the BHTC is illustrated in Fig. 5. The best overlap is reported between the experimental data and the models (*Stephan and Körner* [38], *Calus and Rice* [39] and *Inoue* [44]).

Fig. 6 shows a significant decrease in the surface tension of the solutions relative to the deionized water due to the increase in isopropanol. The reduction in the surface tension for isopropanol of 20 V.% and 80 V.% were obtained as 18.455% and 47.709%, respectively. The isopropanol imposes on the solution a decreasing surface tension along with increasing the volatility that causes large changes in two parameters of the bubble departure diameter and

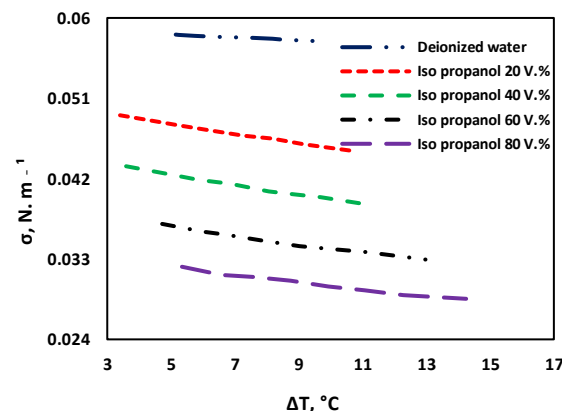


Fig. 6: The variations of the surface tension in the solutions.

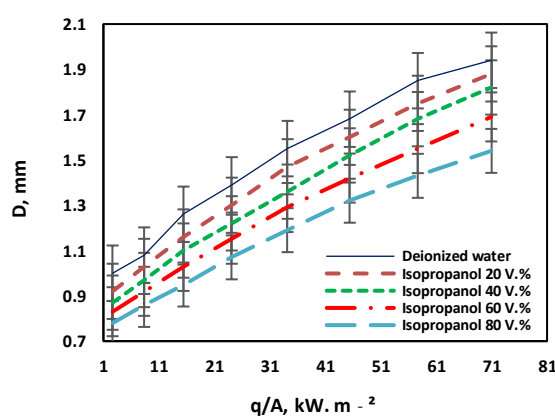
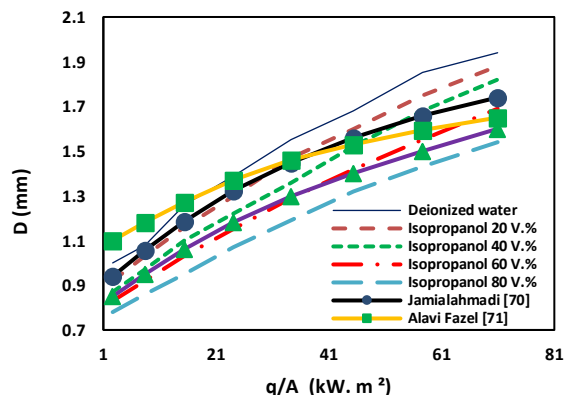


Fig. 7: The bubble departure diameter of the solutions.

bubble departure frequency. Reducing the surface tension leads to a decrease in the residence time and consequently the bubble growth decreases. The bubble departure diameter of the solutions is shown in Fig. 7.

In general, reduction in the size of the bubble departure diameter makes a decrease in the mixing and fluctuations of the process. The bubble departure diameter plays a significant role in increasing the heat transfer coefficient of the pool boiling. On the other hand, the larger bubbles separate more energy from the heat transfer surface and finally its temperature decreases (cooling process). Fig. 8 verifies the validation of the bubble departure diameter with conventional models. Although the two parameters of bubble departure frequency and active nucleation sites density also contribute in increasing the fluctuation state, the bubble departure diameter has the greatest effect. Fig. 9 demonstrates the bubble departure frequency of the solution.

This figure shows that as the concentration of the isopropanol increases, the bubble departure frequency



**Fig. 8:** The bubble departure diameter's validation of the solutions.

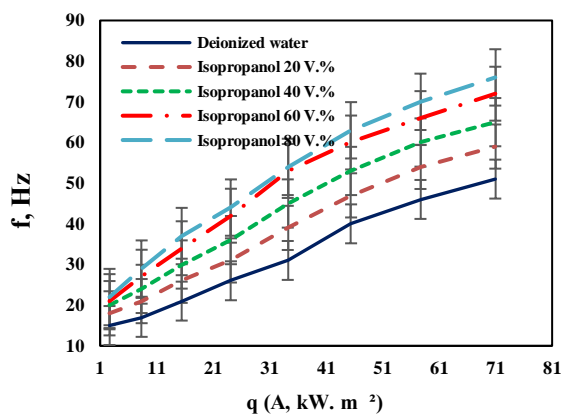


**Fig. 9:** The bubble departure frequency of the solutions.

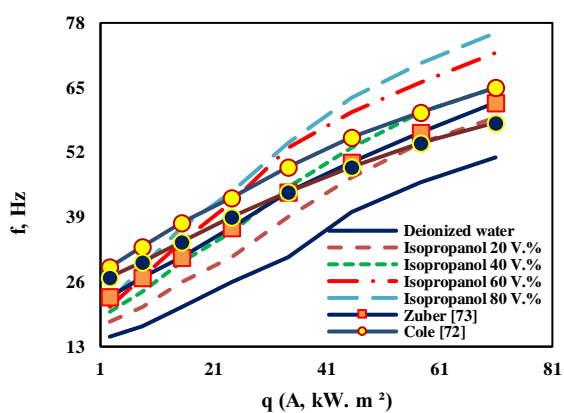


**Fig. 10:** The bubble departure frequency's validation of the solutions.

increases sharply. The maximum increase was 79.154% than deionized water. It was attained at highest concentration ( 80 V.%). The validation of the experimental data are confirmed in Fig. 10. Despite the

significant increase in bubble departure frequency, the bubble departure diameter decreases sharply (Fig. 7). Therefore, the frequency's effect is weaker than the bubble departure diameter in increasing the BHTC. It is verified that the bubble departure frequency has an inverse relation to the bubble departure diameter [25, 51]. Fig. 11 depicts a real image of bubble size changes at different solutions.

As mentioned above, due to the reduction in surface tension, the residence time of the produced bubbles on the heat transfer surface is greatly reduced, and as a result, the bubbles are separated quickly with a smaller diameter. However, increasing the bubble departure frequency at low heat fluxes (beginning of the process) along with decreasing the viscosity of the isopropanol solutions (Fig. 12), increases the BHTC. Because the bubble departure diameter in low heat fluxes is larger and along with increasing the frequency causes a high agitation.

Concerning the figure, the change in the concentration could not significantly increase the active nucleation sites' density. Because active nucleation sites greatly increase with the surface's roughness and heat load from the heat transfer surface [52]. It also changes due to surface's slope [53-55].

#### Introducing a GA based correlation and comparison with conventional ones

Due to many complex mathematical models that has been utilized for the prediction of heat transfer coefficient (Appendix A), it was necessary to find some models that were simple, easy to calculate and fast response with high accuracy. Therefore, in this work, firstly the experimental data were developed through powerful numerical methods of GA optimizer and secondly, the appropriate and optimized model was compared to mathematical models that were close to the experimental conditions, such as *Palen* [37], *Stephan and Körner* [38], *Unal* [41], *Fujita* [43] and *Inoue* [44]. GA optimizer novel correlations was employed to predict the heat transfer coefficient based on power-law correlations (Eq. 8). The ranges of experimental data were used according to Table 2. Afterwards optimizing process, the correlation constants were found at appropriate levels due to the objective function and constraints. Finally, the performance functions were studied. the Absolute Average Deviation (AAD) of 0.0288 and coefficient determination ( $R^2$ ) of 0.968 were reported (Appendix B). The following equation introduces the power-law correlations.

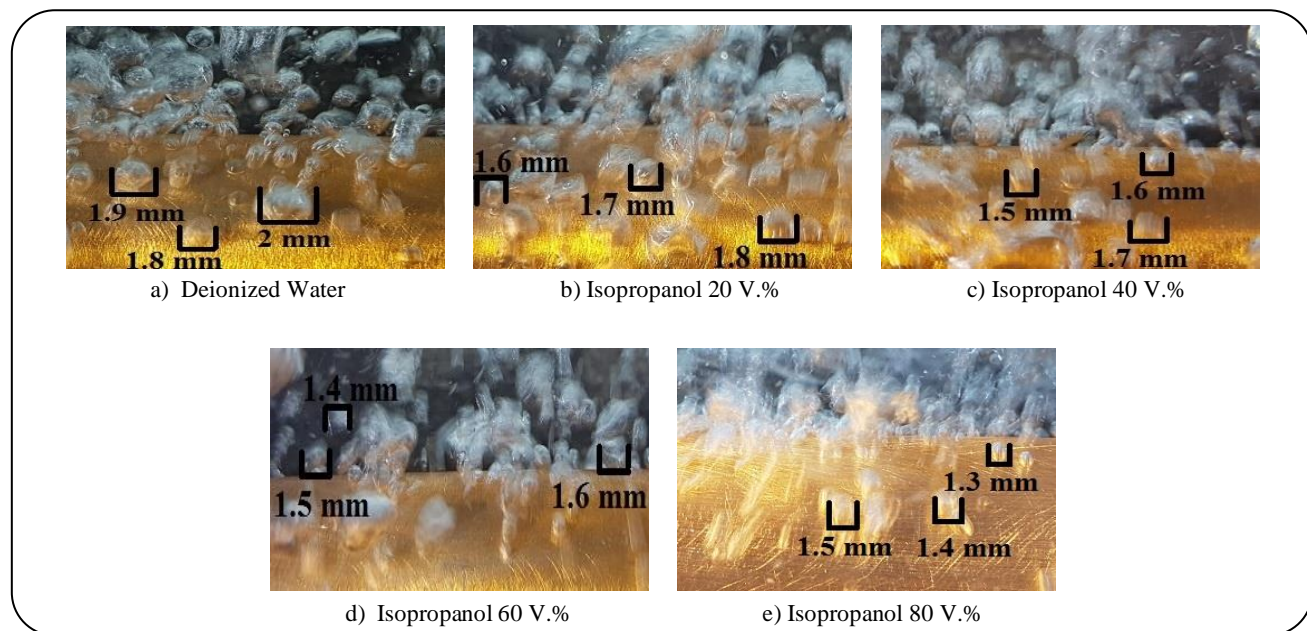


**Fig. 11:** The real image of bubble size at different solutions ( $51 \text{ kW/m}^2$ ).

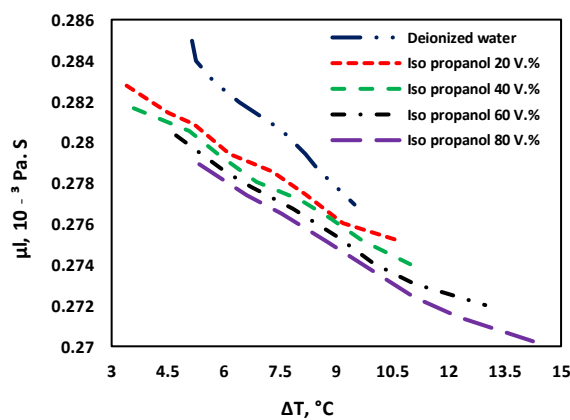


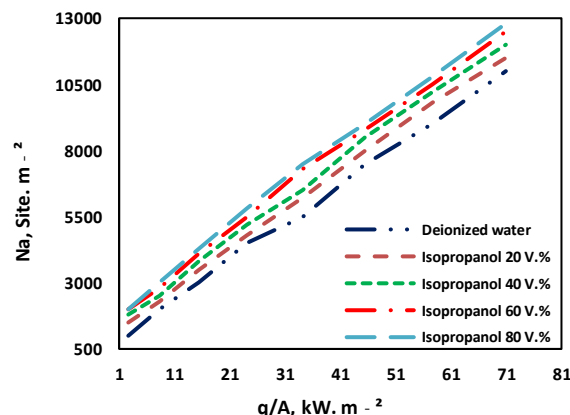
**Fig. 12:** Viscosity changes in the solutions.

Finally, Fig.13 shows the effects of concentration change on the active nucleation sites density.

$$h = \left( \frac{q \times I^*}{k_l \times T_{\text{bulk}}} \right)^{0.705} \times \left( \frac{\alpha'^2 \times \rho_l}{\sigma_{\min} \times I^*} \right)^{-0.045} \times \left( \frac{C_{Pl} \times T_{\text{bulk}} \times I^{*2}}{\alpha'^2} \right)^{0.467} \times \left( \frac{h_{fg} \times I^{*2}}{\alpha'^2} \right)^{-0.399} \times \left( \frac{\rho_v}{\rho_l} \right)^{-0.168} \quad (10)$$

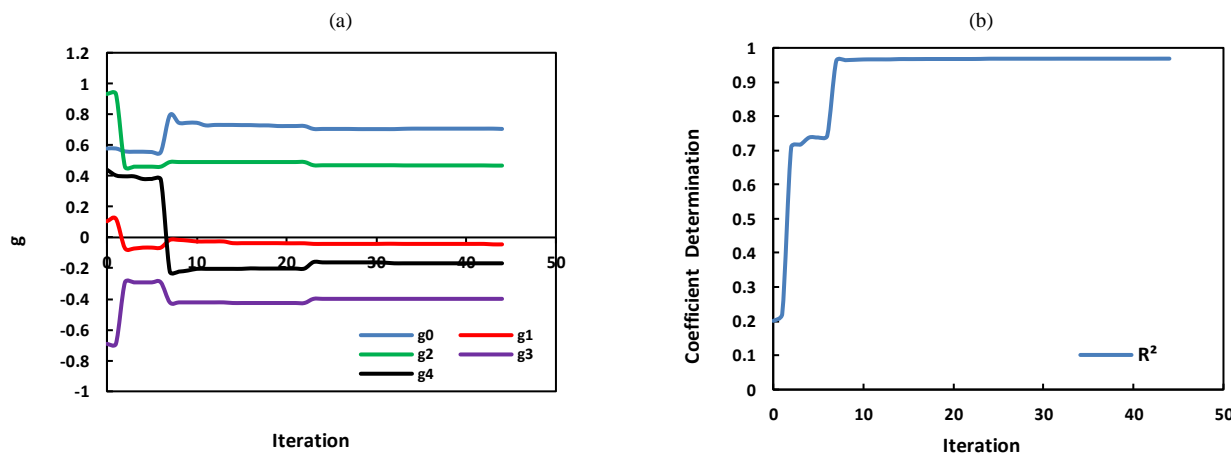
The procedures for coefficient determination and the constants to reach a convergent response are shown in Fig. 14 (a,b), respectively. This figure confirms validation and convergent response of the optimization procedure.

Fig. 15 illustrates a comparison with the present model and other conventional ones. The results revealed



**Fig. 13:** The active nucleation sites of the solutions.

that the heat transfer coefficient's outputs were well forecasted by the GA. In addition, this figure demonstrates the validation of the models through the present work. It can be seen that the GA predicts the heat transfer coefficient data better than others. In addition, TheUnal model with an AAD of 0.0641 showed a good performance after the GA. Subsequently, the Palen and Fujita models presented a similar approach (AAD of 0.1010 and 0.1000, respectively). Finally, the Inoue and Stephan models (AAD of 0.2726 and 0.3389, respectively) revealed weak applications in predicting the heat transfer coefficient and had not a good agreement with the experimental data.



*Fig. 14: Convergent responses of the GA; a. the coefficient determination, b. the model constants.*

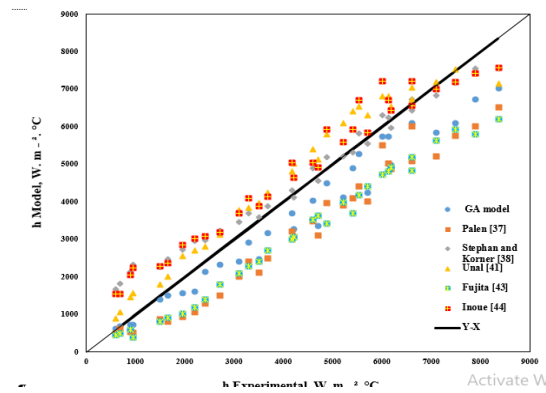


*Fig. 15: Comparison of the GA based correlation with conventional models.*

## CONCLUSIONS

In the present work, we tried to study the effects of the bubble dynamics on the heat transfer coefficient in the pool boiling process. The experiments were carried out using isopropanol solutions. With increasing concentration of isopropanol solutions, bubble departure frequency and active nucleation sites increased while the bubble departure diameter decreased. Decreasing surface tension and viscosity can be reasons for this claim. The concentration of 20 V.% was determined as an optimum state and bubble departure diameter presented a prominent effect. Therefore it could make a turbulent situation and followed by an increase in the heat transfer coefficient. In order to prevent errors in calculating the heat transfer coefficient due to past conventional models, it was attempted to use a numerical model of artificial intelligence. The GA approach played a significant role

in reducing the time and cost of experiments. This method had a good agreement with the experimental data in comparison with the conventional models. As a conclusion, the GA based correlation can be used as general model in related industries.

## Nomenclatures

A	Area, m <sup>2</sup>
C <sub>P</sub>	Heat capacity, J/kg.°C
C <sub>r</sub>	Fixed coefficient of Rohsenow equation
D	Bubble departure diameter, mm
D <sub>AB</sub>	Penetration factor, m <sup>2</sup> /s
f	Bubble departing frequency, Hz
F <sub>P</sub>	Parameter of Mostinski equation
f <sub>w</sub>	Parameter of Jabardo equation
h	Heat transfer coefficient, W/m <sup>2</sup> °C
H <sub>fg</sub>	Specific heat of vaporization, J/kg
I	Current, A
I*	Parameter of Kutateladze equation
K	Thermal conductivity, W/m. °C
K <sub>o</sub>	Parameter of Stephan and Körner equation
L	Length (Cylindrical), cm
M*	Parameter of Kutateladze equation
M <sub>W</sub>	Molecular weight, kg/kmol
N <sub>a</sub>	Active nucleation sites density, 1.m <sup>2</sup>
P	Pressure, Pa
Q	Heat, W
R <sub>a</sub>	Roughness average, μm
R <sub>ao</sub>	Average roughness of baseline
S	Surface
T	Temperature, °C

$g_c$	Correction coefficient of incompatible units, $\frac{Lb_m ft}{Lb_f S^2}$	$\varphi$	Phase difference between voltage and electrical current Difference
$V$	Voltage, V	$\Delta$	
$W$	Watt, W		
$X$	Liquid mole fraction	<b>Subscripts or superscripts</b>	
$Y$	Steam mole fraction	0	Base
		b	Bubble
		bp	Boiling point
		c	Critical
		g	Growing
		l	Liquid
		id	Ideal
		r	Reduced
		sat	Saturation
		th	Thermometers
		v	Vapor

**Greek symbols**

$\hat{\alpha}$	Thermal diffusivity, $m^2/s$
$\beta'$	Fixed coefficient of Rohsenow equation
$\Delta$	Heat penetration depth, m
$P$	Density, $kg/m^3$
$\mu$	Viscosity, $kg.m.s$
$\sigma$	Surface tension, N/m
$\pi$	Pi number

**APPENDIX A***The proposed relations of the researchers to the heat transfer coefficient.*

Reference	Correlation	Solution
Rohsenow [20]	$\frac{h\beta'}{K} \left[ \frac{gc\sigma}{g(\rho_l - \rho_v)} \right]^{\frac{1}{2}} = C_f \left[ \frac{\beta'}{\mu} \left( \frac{g_c \sigma}{g(\rho_l - \rho_v)} \right)^{\frac{1}{2}} \frac{w}{A} \right]^{\frac{2}{3}} \left( \frac{C_H}{k} \right)^{-0.7}$	Pure liquid
McNelly [56]	$h=0.225 \left( \frac{q_c p_l}{A H f_g} \right)^{0.69} \left( \frac{p k L}{\sigma} \right)^{0.31} \left( \frac{\rho_l}{\rho_v} - 1 \right)^{0.33}$	Pure liquid
Kutateladze [57]	$h=[3.37E-9 \frac{KL}{I^*} \left( \frac{H f_g}{CPI(\frac{q}{A})} \right)^{-2} M^{-4}]^{\frac{1}{3}}, \quad I^*=\left[ \frac{\sigma}{g(\rho_l - \rho_v)} \right]^{0.5}, \quad M^*^{-4}=\frac{(\frac{p}{\rho_v})^2}{\frac{\sigma g}{\rho_l - \rho_v}}$	Pure liquid
Mostinski [58]	$h=(3.596E-5)Pc^{0.69} \left( \frac{q}{A} \right)^{0.7} F_p$	Pure liquid
Labantsov [59]	$h=0.075[1+10(\frac{\rho_v}{\rho_l - \rho_v})^{0.67}] \left[ \frac{k l^2}{v \sigma (T_{s \text{ sat}} + 273.15)} \right]^{0.33} \left( \frac{q}{A} \right)^{0.67}$	Pure liquid
Boyko-Kruzhiline [60]	$h=0.082 \frac{k l}{I^*} \left[ \frac{H f_g (\frac{q}{A})}{g(T_s + 273.15) k l} \left( \frac{\rho_v}{\rho_l - \rho_v} \right) \right]^{0.7} \left[ \frac{T_{s \text{ sat}} + 273.15 c_p l \sigma p}{H f_g^2 \rho v^2 I^*} \right]^{0.33}$	Pure liquid
Stephan and Abdelsalam [21]	$\frac{hd_b}{kl} = (0.24E + 7) \left( \frac{qd_b}{Ak_l} \right)^{0.673} \left( \frac{H_{fg} d_b^2}{K_l^2} \right)^{-1.58} \left( \frac{T_{sat} d_b C_{pl}}{K_l^2} \right)^{1.26} \left( \frac{\rho_l - \rho_v}{\rho_l} \right)^{5.22}$	Pure liquid
	Refrigerant cycle for ammonia and fluids $\frac{hd_b}{kl} = 267 \left( \frac{qd_b}{Ak_l T_{sat}} \right)^{0.745} \left( \frac{\rho_v}{\rho_l} \right)^{0.581} \left( \frac{\alpha_l}{kl} \right)^{0.533}$	
	The general form of the equation $\frac{hd_b}{kl} = 0.23 \left( \frac{qd_b}{Ak_l T_{sat}} \right)^{0.647} \left( \frac{\rho_v}{\rho_l} \right)^{0.297} \left( \frac{H_{fg} d_b^2}{\alpha^2} \right)^{0.371} \left( \frac{\rho_l \alpha^2}{\sigma d_b} \right)^{0.35} \left( \frac{\rho_l - \rho_v}{\rho_l} \right)^{-1.73}$	
Nishikawa [61]	$h=\frac{31.4 p_c^{0.2}}{mw^{0.1} T_c^{0.9}} (8R_a)^{0.2} \left( 1 - \frac{p}{p_c} \right) \left( \frac{p}{pc} \right)^{0.23} \left( q/A \right)^{0.8} \left[ 1 - 0.99(p/p_c) \right]^{0.9}$	Pure liquid
Cooper [62]	$h=55 p_r^{0.12-0.443 R_p} (-\log p_r)^{-0.55} mw^{-0.5} (q/A)^{0.67}$	Pure liquid
Fujita [63]	$h=1.21(q/A)^{0.83}$	Pure liquid
Gorenflo [64]	$\frac{h}{h_0} = \left( \frac{q}{q_0} \right)^n (p_r) F(p_r) \left( \frac{R_a}{R_{a0}} \right)^{0.133}$	Pure liquid

**The proposed relations of the researchers to the heat transfer coefficient.**

Sarma [65]	$h = \frac{k}{D} \left( \frac{q''}{3.8 \times 10^{-6} \mu_i h_{fg}} \sqrt{\frac{\sigma}{g(\rho_l - \rho_v)}} P_r^{0.72} \left( \frac{\rho_D}{\mu_i h_{fg}^{0.5}} \right)^{-0.55} \left( \frac{\sigma}{g D^2 (\rho_l - \rho_v)} \right)^{-0.825} \right)^{\frac{1}{1.22}}$	Pure liquid
Jabardo [66]	$h = (q/A)^m f_w P_r^{0.45} [-\log(P_r)]^{-0.8} R_a^{0.2} Mw^{-0.5}, \quad m = 0.9-0.3 P_r^{0.2}$	Pure liquid
Alavi Fazel [67]	$h = \frac{3.253 \sigma^{0.125} H_{fg}^{0.125} (q/A)^{0.876}}{T_{sat} \bar{\alpha}^{0.145}}$	Pure liquid
Igor Seicho [68]	$h = 154 \left[ \left( \frac{C_{pl} T_{sat}}{h_{lv}} \right)^{1.72} \left( \frac{C_{pl} \mu_l}{K_l} \right)^{-0.34} \left( \frac{d_b q''}{\mu_l h_{lv}} \right)^{0.62} \left( \frac{S}{L_b} \right)^{-0.05} \right] \times \frac{k_l}{L_b} \quad 1 \text{mm} > S > 0.1 \text{mm}$	Pure liquid
Palen [37]	$\frac{h}{h_{id}} = e^{-[0.027 \Delta T_{bp}]}$	Mix liquid
Stephan and Körner [38]	$\frac{h}{h_{id}} = \frac{1}{1 + K_0  y - x  (0.88 + 0.13 P)} \quad K_0 = -1.141 \log(P^*) - 0.06$	Mix liquid
Calus and Rice [39]	$\frac{h}{h_{id}} = \frac{1}{\left[ 1 +  y - x  \left( \frac{\bar{\alpha}}{D_{AB}} \right)^{0.50} \right]^{0.7}}$	Mix liquid
Schlunder [40]	$\frac{h}{h_{id}} = \left\{ 1 + \frac{h_{id}}{q} \left[ \sum_{i=1}^{n-1} (T_{Si} - T_{Si}) (y_i - x_i) \left( 1 - \exp \left( \frac{-B_o q}{\beta_{li} \rho_l H_{fg}} \right) \right) \right] \right\}^{-1}$ $B_0 = 1 \quad ; \quad \beta_l = 2E - 4 \text{ m/s}$	Mix liquid
Thome [42]	$\frac{h}{h_{id}} = \left[ \frac{1}{1 + \frac{h_{id} \Delta T_{bp}}{q} \cdot \left[ 1 - \exp \left( \frac{-B_o q}{\beta_{li} \rho_l H_{fg}} \right) \right]} \right]$	Mix liquid
Unal [41]	$\frac{h}{h_{id}} = \frac{1}{[1 + (b_2 + b_3)(1 + b_4)][1 + b_5]}$ $b_2 = (1 - x) \ln \frac{1.01 - x}{1.01 - y} + x \ln \frac{x}{y} +  y - x ^{1.5}$ $\frac{x}{y} - 1 \text{ for } x = y = 0$ $b_3 = 0; \quad b_4 = 152 P_r^{3.9} b_5 = 0.92  y - x ^{0.001} P_r^{0.66}$	Mix liquid
Fujita [43]	$\frac{h}{h_{id}} = \frac{1}{1 + \frac{h_{id} \Delta T_{bp}}{q} \left[ 1 - 0.75 \exp \left[ \left( \frac{-60q}{\rho_v h_{fg}} \right) \cdot \left( \frac{\rho_v^2}{\sigma g (\rho_l - \rho_v)} \right)^{\frac{1}{4}} \right] \right]}$	Mix liquid
Inoue [44]	$\frac{h}{h_{id}} = \frac{1}{1 + \frac{h_{id} \Delta T_{bp}}{q} \left[ 1 - 0.75 \exp \left( -\frac{0.75q}{10^5} \right) \right]}$	Mix liquid
Vinayak [45]	$\frac{h}{h_{id}} = \left[ 1 - \left(  y - x  \sqrt{\frac{D_{AB}}{\bar{\alpha}}} \right) \right]$	Mix liquid
Alavi Fazel [46]	$\frac{h}{h_{id}} = \frac{1}{1 + \frac{\Delta T_{bp}}{\Delta T_{id}} (1 - \exp(-1.646 \times 10^{-2} \left( \frac{q}{A} \right)))}$	Mix liquid

## APPENDIX B Performance functions.

$$AAD = \frac{1}{N} \sum_{i=1}^N \left( \frac{y_{exp,i} - y_{model,i}}{y_{exp,i}} \right)^2 \quad (11)$$

$$R^2 = \frac{\sum_{i=1}^N (y_{exp,i} - y_{model,mean})^2 - \sum_{i=1}^N (y_{exp,i} - y_{model,i})^2}{\sum_{i=1}^N (y_{model,mean} - y_{exp,i})^2} \quad (12)$$

Received : Sep. 6, 2021 ; Accepted : Feb. 14, 2022

## REFERENCES

- [1] Nasr R., Rahaei N., Improving Heat Transfer in Falling Film Evaporators in Food Industries, *Iran. J. Chem. Chem. Eng. (IJCCE)*, **38**: 237-250 (2019).
- [2] Yim K., Lee J., Naccarato B., Kim K.J., Surface Wettability Effect on Nucleate Pool Boiling Heat Transfer with Titanium Oxide ( $TiO_2$ ) Coated Heating Surface, *Int. J. Heat Mass Transfer*, **133**: 352-358 (2019).

- [3] Alavi F.S., Jami A.M., Seyf K.A., **Experimental Investigation in Pool Boiling Heat Transfer of Pure/Binary Mixtures and Heat Transfer Correlations**, *Iran. J. Chem. Chem. Eng. (IJCCE)*, **27**: 135-150 (2008).
- [4] Liang G, Mudawar I., **Review of Pool Boiling Enhancement by Surface Modification**, *Int. J. Heat Mass Transfer*, **128**: 892-933 (2019).
- [5] Kumar G.U., Suresh S., Thansekhar M., Halpati D., **Role of Inter-Nanowire Distance in Metal Nanowires on Pool Boiling Heat Transfer Characteristics**, *Journal of Colloid and Interface Science*, **532**: 218-230 (2018).
- [6] Wang J., Diao M., Liu X., **Numerical Simulation of Pool Boiling with Special Heated Surfaces**, *Int. J. Heat Mass Transfer*, **130**: 460-468 (2019).
- [7] Mohammadi N., Fadda D., Choi CK., Lee J., You S., **Effects of Surface Wettability on Pool Boiling of Water Using Super-Polished Silicon Surfaces**, *Int. J. Heat Mass Transfer*, **127**: 1128-1137 (2018).
- [8] Gheithaghy A.M., Saffari H., Zhang G.Q., **Effect of nanostructured microporous surfaces on pool boiling augmentation**, *Heat Transfer Engineering*, **40**: 762-771 (2019).
- [9] Esawy M., Malayeri M., **Modeling of CaSO<sub>4</sub> Crystallization Fouling of Finned Tubes During Nucleate Pool Boiling**, *Chemical Engineering Research and Design*, **118**: 51-60 (2017).
- [10] Gouda R.K., Pathak M., Khan M.K., **Pool Boiling Heat Transfer Enhancement with Segmented Finned Microchannels Structured Surface**, *Int. J. Heat Mass Transfer*, **127**: 39-50 (2018).
- [11] Sur A., Lu Y., Pascente C., Ruchhoeft P., Liu D., **Pool Boiling Heat Transfer Enhancement with Electrowetting**, *Int. J. Heat Mass Transfer*, **120**: 202-217 (2018).
- [12] Khooshehchin M., Fathi S., Salimi F., Ovaysi S., **Investigation of Effects of Heater Tube Angle on the Pool Boiling Heat Transfer Coefficient**, *Iran. J. Chem. Chem. Eng. (IJCCE)*, **154**: 119783 (2021).
- [13] Godinez J.C., Fadda D., Lee J., You S.M., **Development of a Stable Boehmite Layer on Aluminum Surfaces for Improved Pool Boiling Heat Transfer in Water**, *Applied Thermal Engineering*, **156**: 541-549 (2019).
- [14] Emery T.S., Jaikumar A., Raghupathi P., Joshi I., Kandlikar S.G., **Dual Enhancement in HTC and CHF for External Tubular Pool Boiling—A Mechanistic Perspective and Future Directions**, *Int. J. Heat Mass Transfer*, **122**: 1053-1073 (2018).
- [15] Wang J., Li F.C., Li X.B., **Bubble Explosion In Pool Boiling Around a Heated Wire in Surfactant Solution**, *Int. J. Heat Mass Transfer*, **99**: 569-575 (2016).
- [16] Kutateladze S., **Hydrodynamic Model of Heat Transfer Crisis In Free-Convection Boiling**, *J. Tech. Phys.*, **20**: 1389-1392 (1950).
- [17] Kutateladze S., **On the Transition to Film Boiling Under Natural Convection**, *Kotloturbostroenie*, **3**: 10-12 (1948).
- [18] Zuber N., **On the Stability of Boiling Heat Transfer**, *Trans Am. Soc. Mech. Engrs.*, **80** (1958).
- [19] Cao Z., Wu Z., Pham A.D., Yang Y., Abbood S., Falkman P., Ruzgas T., Albèr C., Sundén B., **Pool boiling of HFE-7200 on Nanoparticle-Coating Surfaces: Experiments and Heat Transfer Analysis**. *Int. J. Heat Mass Transfer*, **133**: 548-560 (2019).
- [20] Rohsenow W.M., **A Method of Correlating Heat Transfer Data for Surface Boiling of Liquids** Cambridge, Mass, *MIT Division of Industrial Cooperation*, (1951).
- [21] Stephan K., Abdelsalam M., **Heat-Transfer Correlations for Natural Convection Boiling**, *Int. J. Heat Mass Transfer*, **23**: 73-87 (1980).
- [22] Xu Z., Zhao C., **Experimental Study on Pool Boiling Heat Transfer in Gradient Metal Foams**, *Int. J. Heat Mass Transfer*, **85**: 824-829 (2015).
- [23] Xu Z., Zhao C., **Enhanced Boiling Heat Transfer by Gradient Porous Metals in Saturated Pure Water and Surfactant Solutions**, *Applied Thermal Engineering*, **100**: 68-77 (2016).
- [24] Sathyabhamma A., **Nucleate Pool Boiling Heat Transfer From a Flat-Plate Grooved Surface**, *J. Enhanced Heat Transfer*, **22** (2015).
- [25] Khooshehchin M, Mohammadidous A, Ghotbinasab S., **An optimization Study on Heat Transfer of Pool Boiling Exposed Ultrasonic Waves and Particles Addition**, *Int. J. Heat Mass Transfer*, **114**: 104558 (2020).

- [26] Shojaeian M., Yildizhan M.M., Coşkun Ö., Ozkalay E., Tekşen Y., Gulgın M.A., Acar H.F.Y., Koşar A., **Investigation of Change In Surface Morphology of Heated Surfaces Upon Pool Boiling of Magnetic Fluids Under Magnetic Actuation**, *Materials Research Express*, **3**: 096102 (2016).
- [27] Abdollahi A., Salimpour M.R., Etesami N., **Experimental Analysis of Magnetic Field Effect on the Pool Boiling Heat Transfer of a Ferrofluid**, *Applied Thermal Engineering*, **111**: 1101-1110 (2017).
- [28] Özdemir M.R., Sadaghiani A.K., Motezakker A.R., Parapari S.S., Park H.S., Acar H.Y., Koşar A., **Experimental Studies on Ferrofluid Pool Boiling in the Presence of External Magnetic Force**, *Applied Thermal Engineering*, **139**: 598-608 (2018).
- [29] Shahriari A., Birbarah P., Oh J., Miljkovic N., Bahadur V., **Electric Field-Based Control and Enhancement of Boiling and Condensation**, *Nanoscale and Microscale Thermophysical Engineering*, **21**: 102-121 (2017).
- [30] Quan X., Gao M., Cheng P., Li J., **An Experimental Investigation of Pool Boiling Heat Transfer on Smooth/Rib Surfaces under an Electric Field**, *Int. J. Heat Mass Transfer*, **85**: 595-608 (2015).
- [31] Jun S., Wi H., Gurung A., Amaya M., You S.M., **Pool Boiling Heat Transfer Enhancement of Water Using Brazed Copper Microporous Coatings**, *Journal of Heat Transfer*, **138**: 071502 (2016).
- [32] Godinez J.C., Fadda D., Lee J., You S.M., **Enhancement of Pool Boiling Heat Transfer in Water on Aluminum Surface with High Temperature Conductive Microporous Coating**, *Int. J. Heat Mass Transfer*, **132**: 772-781 (2019).
- [33] Guglielmini G., Misale M., Schenone C., **Boiling of Saturated FC-72 on Square Pin Fin Arrays**, *International Journal of Thermal Sciences*, **41**: 599-608 (2002).
- [34] McNeil D., Raeisi A., Kew P., Bobbili P., **A comparison of Flow Boiling Heat-Transfer in In-Line Mini Pin Fin and Plane Channel Flows**, *Applied thermal engineering*, **30**: 2412-2425 (2010).
- [35] Dadjoo M., Etesami N., Esfahany M.N., **Influence of Orientation and Roughness of Heater Surface on Critical Heat Flux and Pool Boiling Heat Transfer Coefficient of Nanofluid**, *Applied Thermal Engineering*, **124**: 353-361 (2017).
- [36] El-Genk M.S., Suszko A., **Effects of Inclination Angle and Liquid Subcooling on Nucleate Boiling on Dimpled Copper Surfaces**, *Int. J. Heat Mass Transfer*, **95**: 650-661 (2016).
- [37] Palen J., Small W., **A New Way to Design Kettle and Internal Reboilers**, *Hydrocarbon Processing*, **43**: 199-208 (1964).
- [38] Stephan K., Korner M., **Calculation of Heat Transfer in Evaporating Binary Liquid Mixtures**, *Chem. Ing. Tech.*, **41**: 409-417 (1969).
- [39] Calus W., Rice P., **Pool Boiling—Binary Liquid Mixtures**, *Chemical Engineering Science*, **27**: 1687-1697 (1972).
- [40] Schlunder E.U., **Heat Transfer in Nucleate Boiling of Mixtures** International Heat Transfer Conference Digital Library Begel House Inc, *International Heat Transfer Conference Digital Library*, (1986).
- [41] Ünal H., **Prediction of Nucleate Pool Boiling Heat Transfer Coefficients for Binary Mixtures**, *Int. J. Heat Mass Transfer*, **29**: 637-640 (1986).
- [42] Thome J., Shakir S., **A New Correlation for Nucleate Pool Boiling of Aqueous Mixtures**, Heat Transfer Conference: Pittsburgh, (1987).
- [43] Fujita Y., Tsutsui M., **Convective Flow Boiling of Binary Mixtures in a Vertical Tube in Convective Flow Boiling**, Taylor & Francis, Washington, (1996).
- [44] Inoue T., Monde M., Teruya Y., **Pool Boiling Heat Transfer in Binary Mixtures of Ammonia/Water**, *Int. J. Heat Mass Transfer*, **45**: 4409-4415 (2002).
- [45] Rao G.V., Balakrishnan A., **Heat Transfer in Nucleate Pool Boiling of Multicomponent Mixtures**, *Exp. Therm. Fluid Sci.*, **29**: 87-103 (2004).
- [46] Alavi F.S, Seyfe K.A., Jami A.M., **Pool Boiling Heat Transfer in Water/Amines Solutions**, *International Journal of Engineering*, **2**: 113-130 (2008).
- [47] Fazel S.A.A., **A Genetic Algorithm-Based Optimization Model for Pool Boiling Heat Transfer on Horizontal Rod Heaters at Isolated Bubble Regime**, *Heat and Mass Transfer*, **53**: 2731-2744 (2017).
- [48] Gorenflo D., **Pool Boiling**, VDI Heat Atlas, VDI-Verlag, Dusseldorf, Germany., (1993).
- [49] Schmitt L.M., **Theory of Genetic Algorithms II: Models For Genetic Operators over the String-Tensor Representation of Populations and Convergence to Global Optima for Arbitrary Fitness Function under Scaling**, *Theoretical Computer Science*, **310**: 181-231 (2004).

- [50] Goldberg D.E., *Genetic Algorithms in Search, Optimization and Machine Learning*, (1989).
- [51] Khooshechin M., Fathi S., Salimi F., Ovaysi S., The Influence of Surfactant And Ultrasonic Processing on Improvement of Stability and Heat Transfer Coefficient of CuO Nanoparticles in the Pool Boiling, *Int. J. Heat Mass Transfer*, **154**: 119783 (2020).
- [52] Ivey H., Relationships between Bubble Frequency, Departure Diameter and Rise Velocity in Nucleate Boiling, *Int. J. Heat Mass Transfer*, **10**: 1023-1040 (1967).
- [53] Ghotbinasab S., Khooshehchin M., Mohammadidoust A., Rafiee M., Salimi F., Fathi S., Comparing the Heat Transfer Coefficient of Copper Sulfate and Isopropanol Solutions in the Pool Boiling Process: Bubble Dynamic and Ultrasonic Intensification, *Chemical Engineering Science*, **237**: 116589 (2021).
- [54] Thorncroft G., Klausner J., Mei R., An Experimental Investigation of Bubble Growth and Detachment in Vertical Upflow and Downflow Boiling, *Int. J. Heat Mass Transfer*, **41**: 3857-3871 (1998).
- [55] Jung S., Kim H., Effects of Surface Orientation on Nucleate Boiling Heat Transfer in a Pool of Water under Atmospheric Pressure, *Nuclear Engineering and Design*, **305**: 347-358 (2016).
- [56] Cole R., Bubble frequencies and Departure Volumes at Subatmospheric Pressures, *AIChE Journal*, **13**: 779-783 (1967).
- [57] McNelly M., A Correlation of Rates of Heat Transfer to Nucleate Boiling of Liquids, *J Imperial College Chem Eng Soc*, **7**: 18-34 (1953).
- [58] Kutateladze S.S., Heat Transfer in Condensation and Boiling, *AEC-tr-3770*, (1959).
- [59] Mostinski I., Application of the Rule of Corresponding States for Calculation of Heat Transfer and Critical Heat Flux, *Teploenergetika*, **4**: 66-71 (1963).
- [60] Labunstov D., Mechanism of Vapor Bubble Growth in Boiling on the Heating Surface, *J. Eng. Phys.*, **6**: 33-39 (1963).
- [61] Boyko L., Kruzhilin G., Heat Transfer and Hydraulic Resistance During Condensation of Steam in a Horizontal Tube and in a Bundle of Tubes, *Int. J. Heat Mass Transfer*, **10**: 361-373 (1967).
- [62] Nishikawa K., Fujita Y., Ohta H., Hitaka S., Effects of System Pressure and Surface Roughness on Nucleate Boiling Heat Transfer, *Mem. Fac. Eng., Kyushu Univ.*, **42**: 95-123 (1982).
- [63] Cooper M., Saturation Nucleate Pool Boiling- A Simple Correlation, *IChemE Symp Ser*, **786** (1984).
- [64] Nishikawa K., Fujita Y., Nucleate Boiling Heat Transfer and its Augmentation, *Advances in Heat Transfer*, **20**: 1-82 (1990).
- [65] Sarma P., Srinivas V., Sharma K., Subrahmanyam T., Kakac S., A Correlation to Predict Heat Transfer Coefficient in Nucleate Boiling on Cylindrical Heating Elements, *International Journal of Thermal Sciences*, **47**: 347-354 (2008).
- [66] Jabardo J.M.S., Ribatski G., Stelute E., Roughness and Surface Material Effects on Nucleate Boiling Heat Transfer From Cylindrical Surfaces to Refrigerants R-134a and R-123, *Exp. Therm. Fluid Sci.*, **33**: 579-590 (2009).
- [67] Fazel S.A., Roumana S., "Pool Boiling Heat Transfer to Pure Liquids", *WSEAS Conference*, USA (2010).
- [68] Kiyomura I.S., Mogaji T.S., Manetti L.L., Cardoso E.M., A Predictive Model for Confined and Unconfined Nucleate Boiling Heat Transfer Coefficient, *Applied Thermal Engineering*, **127**: 1274-1284 (2017).
- [69] Lee H.C., OhB.Do., BaeS.W., KimM.H., Single Bubble Growth in Saturated Pool Boiling on a Constant Wall Temperature Surface, *International Journal of Multiphase Flow*, **29**: 1857-1874 (2003).
- [70] Jamialahmadi M., Helalizadeh A., Müller-Steinhagen H., Pool Boiling Heat Transfer to Electrolyte Solutions, *Int. J. Heat Mass Transfer*, **47**: 729-742 (2004).
- [71] Fazel S.A.A., Shafaei S.B., Bubble Dynamics For Nucleate Pool Boiling of Electrolyte Solutions, *Journal of Heat Transfer*, **132**: 081502 (2010).
- [72] Cole R., A Photographic Study of Pool Boiling in the Region of the Critical Heat Flux, *AIChE Journal*, **6**: 533-538 (1960).
- [73] Zuber N., Nucleate Boiling. the Region of Isolated Bubbles and the Similarity with Natural Convection, *Int. J. Heat Mass Transfer*, **6**: 53-78 (1963).